EUROPEAN UROLOGY OPEN SCIENCE 38 (2022) 60–66

available at www.sciencedirect.com
journal homepage: www.eu-openscience.europeanurology.com

European Association of Urology

Surgery in Motion: Open Science

Identification of Recurrent Anatomical Clusters Using Three-dimensional Virtual Models for Complex Renal Tumors with an Imperative Indication for Nephron-sparing Surgery: New Technological Tools for Driving Decision-making

Daniele Amparore [a,b], *Federico Piramide* [a], *Angela Pecoraro* [a,b], *Paolo Verri* [a], *Enrico Checcucci* [c,d], *Sabrina De Cillis* [a], *Alberto Piana* [a], *Giovanni Busacca* [a], *Matteo Manfredi* [a], *Cristian Fiori* [a], *Francesco Porpiglia* [a,*]

[a] *Department of Urology, San Luigi Gonzaga Hospital, University of Turin, Orbassano, Turin, Italy;* [b] *European Association of Urology Young Academic Urologists Renal Cancer Working Group, Arnhem, The Netherlands;* [c] *Department of Surgery, Candiolo Cancer Institute, FPO-IRCCS, Candiolo, Turin, Italy;* [d] *European Association of Urology Young Academic Urologists Uro-technology and SoMe Working Group, Arnhem, The Netherlands*

Article info

Article history:
Accepted February 11, 2022

Associate Editor:
M. Carmen Mir

Keywords:
Three-dimensional imaging
Robotic surgery
Nephron-sparing surgery
Kidney cancer
Surgical anatomy

Abstract

Background: Some renal tumors have an imperative indication for nephron-sparing surgery (NSS), such as in cases of chronic kidney disease and bilateral complex tumors.
Objective: To demonstrate the degree to which three-dimensional virtual model (3DVM) assistance can be helpful in planning the surgical strategy for high-complexity renal masses with an imperative indication for NSS.
Design, setting, and participants: Three patients with high-complexity renal masses with unusual anatomy and an imperative indication for NSS were prospectively selected across 2020 and 2021 at our institution. All patients underwent contrast-enhanced computed tomography from which a 3DVM was obtained.
Surgical procedure: Robot-assisted partial nephrectomy with 3DVM augmented reality guidance.
Measurements: Demographics and tumor-related features were recorded. Data for intraoperative, pathological, and functional assessments were collected for all three patients.
Results and limitations: Two of the three patients harbored bilateral renal tumors. The third patient presented with a renal mass in the left kidney and contralateral renal hypoplasia (right-split renal function of 25%). All of the patients demonstrated similar anatomical and tumor features on 3DVMs, with potentially independent vascularization and drainage for the lower pole. In one patient the upper pole of the kidney was spared, exiting in a functionally excluded hydrocalyx, while in the other two cases the upper pole was removed together with the lesion.

* Corresponding author. Department of Urology, San Luigi Gonzaga Hospital, University of Turin, Orbassano, Turin, Italy. Tel. +39 011 9026485; Fax: +39 011 9026244.
E-mail address: porpiglia@libero.it (F. Porpiglia).

https://doi.org/10.1016/j.euros.2022.02.006
2666-1683/

The spared portion of the kidney retained vascularization, as demonstrated by intraoperative ultrasound and indocyanine green injection. The small sample size and short follow-up are the main limitations of the study.
Conclusions: 3DVMs, especially for complex renal masses with an imperative indication for NSS, allow planning of the surgical strategy on the basis of the anatomical characteristics of the organ in which the tumor is growing.
Patient summary: Three-dimensional models help in defining the best surgical strategy for kidney tumors, especially for complex tumors that require surgery to spare as much of the kidney as possible.

1. Introduction

Most nephron-sparing surgery (NSS) procedures are currently performed as primary surgeries in the elective setting on kidneys with a relatively normal anatomy [1,2]. However, in some cases the indication for NSS is imperative, such as a congenital or acquired single kidney, moderate to advanced chronic kidney disease, and bilateral tumors [3,4].

The development and increasing use of robotic surgery and new technologies continue to extend NSS indications, even for cases previously considered too complex or technically difficult for conservative treatment, thanks to careful and timely surgical planning [5–7].

Hyperaccuracy three-dimensional virtual models (3DVMs) of the kidney and tumor anatomy, which are based on preoperative computed tomography (CT) images, have been introduced to improve surgical planning and intraoperative navigation assistance and use different supports that range from holograms to intraoperative superimposition with augmented reality (AR) technology [8–10]. It has been shown that these tools can improve perioperative and functional outcomes in cases involving highly complex renal tumors by optimizing many surgical steps of the procedure [11,12].

For example, with the aid of 3DVMs it is possible to consider the vascular anatomy and possible variants and the morphology of the collecting system simultaneously and assess their relative relationships to the tumor. This allows the surgeon to identify recurrent anatomical “clusters” for which the surgical strategy can be modulated on the basis of the anatomy of the whole organ. In this setting, since the ultimate goal of NSS is to maximally spare renal function, the postoperative result is planned on a future functional rather than a morphometric (ie, tumor anatomy) basis.

The aim of this study was to demonstrate the degree to which 3DVM assistance can help in planning a surgical strategy by considering the effective potential function of the organ instead of focusing on excision of the tumor.

2. Patients and methods

For this study, three challenging clinical cases involving high-complexity renal masses with an imperative indication for NSS were selected.

2.1. *Patient selection*

We considered prospectively maintained data for patients with a radiological diagnosis of a complex renal mass with an imperative indication for NSS who underwent robot-assisted partial nephrectomy (RAPN) at our center across 2020 and 2021. Specifically, three challenging clinical cases with an imperative indication for NSS underwent transperitoneal RAPN performed by a single surgeon (F.P.) with expertise in minimally invasive renal surgery (>500 procedures completed).

The study was conducted in accordance with good clinical practice guidelines, and informed consent was obtained from the patients. According to Italian law (Agenzia Italiana del Farmaco Guidelines for Observational Studies, March 20, 2008), no formal institutional review board or ethics committee approval was needed.

2.2. *Hyperaccuracy 3DVM*

Contrast-enhanced CT images in digital DICOM format were processed by MEDICS Srl (www.medics3d.com) using dedicated software for hyperaccuracy 3D (HA3D) virtual reconstruction of the case, as previously reported [9–12]. In brief, the reconstruction was focused on the kidney vasculature and collecting system, the kidney parenchyma, and the renal mass. The renal pedicle, including both the arterial and venous trees, was reconstructed using the dynamic region growing method. The urinary collecting system was reconstructed using the same method for the excretory phase of urography CT scans. The renal parenchyma was segmented using selective thresholding, separating different voxels and grouping them by a grayscale. The next step was the creation of a mathematical 3D model and a corresponding interactive 3D pdf file. After reconstructing the anatomy of both the kidney and the pathological renal mass, the renal vasculature and urinary collecting system were carefully evaluated. Virtual navigation for the HA3D model allowed the surgeon to appreciate the anatomical details of the complex renal mass, focusing on its relationships with the vascular arterial and venous vessels arising from the aorta and the inferior vena cava, and with the intrarenal portion of the urinary collecting system. Of note, navigation of the 3D pdf file after HA3D model rendering allowed careful evaluation of the preoperative surgical strategy by the whole surgical team.

2.3. *Planning and surgical procedures*

2.3.1. *Case 1*

Case 1 was a 50-yr-old male harboring an 80-mm right central renal mass with a PADUA score of 13 incidentally detected on a preoperative CT scan with contralateral kidney hypoplasia (Fig. 1A) identified on a preoperative renal scan (split renal function [SRF] of 25%). The surgical indication was imperative right NSS.

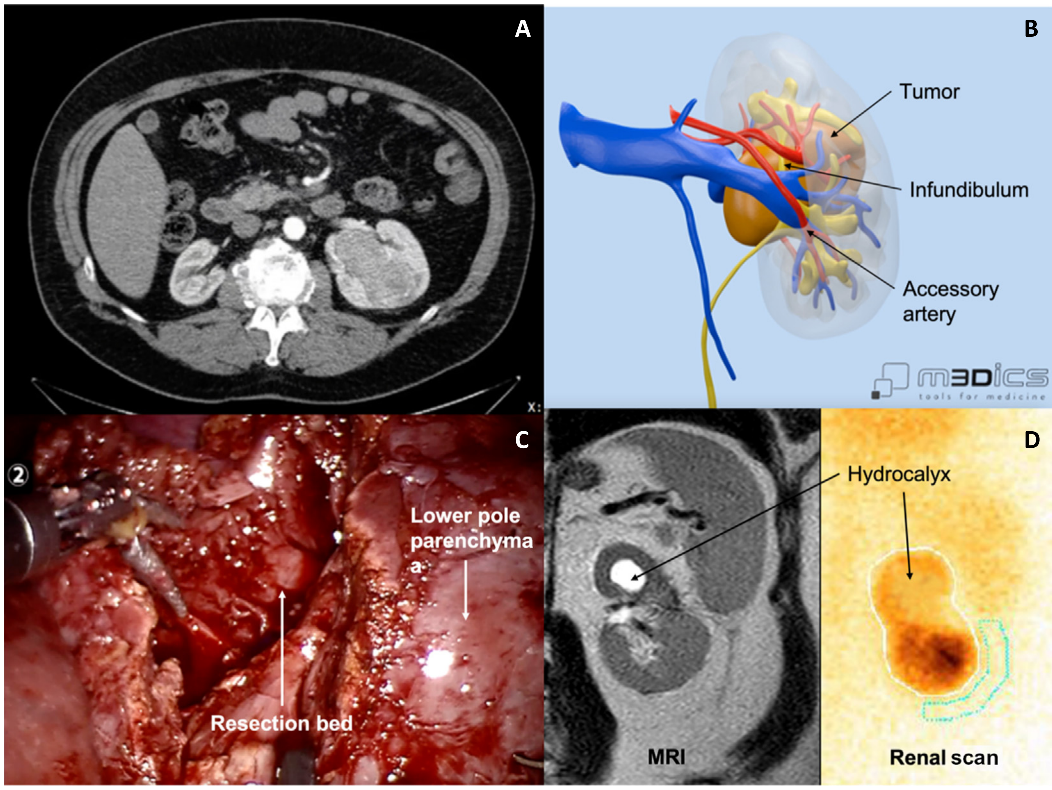

Fig. 1 – (A) Preoperative computed tomography scan and (B) three-dimensional virtual for case 1. (C) Intraoperative tumor resection bed after robot-assisted partial nephrectomy. (D) At 3 mo after surgery, contrast-enhanced magnetic resonance imaging (MRI) and a renal scan of the operated kidney showed a non–contrast enhancing upper pole with a hydrocalyx not draining urine in the renal pelvis.

A preoperative 3DVM showed that the infundibulum of the upper calyceal group was dislocated by the tumor, while an accessory artery fed the lower pole of the kidney (Fig. 1B). In this case an attempt of enucleoresection was planned. After exposure of the kidney surface, the 3D model was superimposed over the real anatomy using AR technology to visualize the tumor location, hidden inside the central portion of the parenchyma. After clamping of the arterial vessels, the edges of the lesion were marked on the renal parenchyma surface and the resection phase was started.

During this phase some tubular structures, assumed to be vessels coming from the medial portion of the sinus and facing the tumor pseudocapsule, were clipped using Absolok [13]. The resection proceeded along the pseudocapsular plane up to the posterior face of the lesion. Then both of the renal poles were spared, with violation of the collecting system at the level of the superior calyx. During the reconstructive phase, the violated calyceal structures were selectively sutured, while a double-layer suture, strengthened with Hem-o-Lok and Absolok clips, was inserted in the resection bed (Fig. 1C).

At 3 mo after surgery, magnetic resonance imaging (MRI) showed a non–contrast enhancing upper pole with a hydrocalyx not draining urine in the renal pelvis. A renal scan confirmed the nonfunctional status of the upper half of the kidney. This suggested the involvement of the infundibular connection to the upper calyceal system, resulting in loss of all of the parenchymal tissue of pertinence (Fig. 1D).

2.3.2. Case 2

Case 2 was a 57-yr-old male harboring bilateral endophytic central renal masses: a 60-mm right mesorenal mass infiltrating the renal sinus and a 70-mm left mesorenal mass dislocating but not infiltrating the intrarenal structures. The PADUA score for both masses was 13 (Fig. 2A). Therefore, the surgical indication was imperative left NSS with synchronous right radical nephrectomy (RN).

As for the previous case, a 3DVM for the left kidney showed that the infundibulum of the upper calyceal group was dislocated by the tumor, with an accessory artery feeding the lower pole of the kidney (Fig. 2B). In this case, considering the structures of the kidney from an “anatomic-f unctional” perspective, the surgical strategy was based on sacrifice of the upper portion of the kidney together with the tumor, maintaining an arterial and venous circle for the lower renal pole together with drainage of the collecting system from the middle and lower calyces to the renal pelvis (Fig. 2C).

After robotic right RN, the patient was placed on his contralateral flank for synchronous robotic left heminephrectomy. The edges of the lesion were marked on the renal parenchyma surface under 3D AR guidance. The main renal artery and renal vein were clamped with bulldog clips. The dissection plane was followed towards the lower face of the tumor. In the medial portion of the renal sinus, the infundibulum draining the upper calyx was identified and clipped with Absolok.

The mesorenal branch of the renal vein was clipped with Hem-o-Lok clips, maintaining the venous drainage from the inferior branch. The main renal artery was also clipped, sparing the accessory artery feeding the lower pole (Fig. 2D). After a double-layer suture of the renal defect and reconstruction of Gerota’s fascia, intraoperative ultrasound confirmed arterial and venous blood flow to the renal remnant. At the end of the procedure, a double-J stent was placed to favor drainage of urine towards the bladder, minimizing the risk of leakages. The stent was removed 1 mo later. After surgery, the patient was treated with dialysis

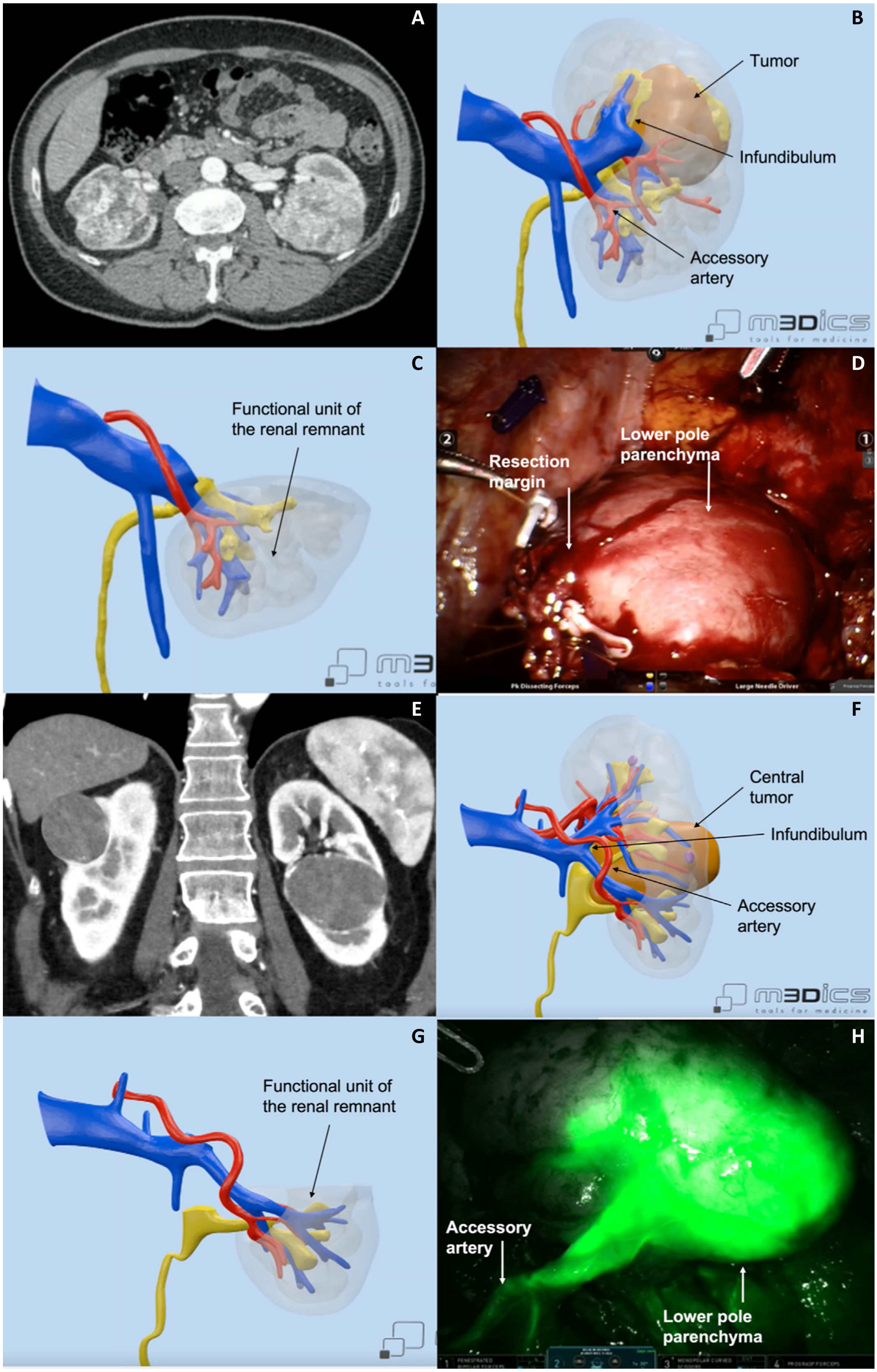

Fig. 2 – (A) Preoperative computed tomography (CT) scan and (B) three-dimensional virtual model for case 2. (C) Three-dimensional virtual model for case 2 showing the surgical strategy based on sparing of the lower pole of the kidney with its vascular and drainage anatomical unit and (D) corresponding intraoperative counterpart. (E) Preoperative CT scan and (F) three-dimensional virtual model for case 3. (G) Three-dimensional virtual model for case 3 showing the surgical strategy based on sparing of the lower pole of the kidney with its vascular and drainage anatomical unit. (H) Intraoperative indocyanine green injection identifying the avascular plane for dissection of the parenchyma.

for 6 mo. At 1 yr, his serum creatinine level was 2.2 mg/dl, with an estimated glomerular filtration rate (eGFR) of 33%. No further dialysis sessions were needed.

2.3.3. Case 3

Case 3 was a 67-yr-old female with bilateral renal masses on a CT scan: an exophytic 45-mm mesorenal mass (PADUA score 9) and a 55-mm central mesorenal mass (PADUA score 13) dislocating, but not infiltrating, the intrarenal structures (Fig. 2E), were identified on the right and left side, respectively. A renal scan revealed SRF of 47% and 53% for the right and left kidney, respectively. The surgical indication was imperative left NSS and metachronous right NSS.

A 3DVM of the left kidney was able to identify an independent anatomic-functional unit at the lower pole, so the surgical strategy was sacrifice of the upper pole and preservation of the lower pole of the kidney with a view to potential functioning after surgery (Fig. 2F,G).

After isolation of the organ, near-infrared fluorescence imaging was used to enhance the portion of the kidney fed by the accessory artery of the lower pole [14]. Indocyanine green (ICG) was used to identify the avascular plane to guide dissection of the parenchyma (Fig. 2H).

The pseudocapsular plane of the tumor was identified and the infundibulum draining the upper and middle calyces was clipped, as well as the mesorenal branch of the renal vein and the main renal artery.

At the end of the reconstructive phase, ICG was injected again to check the arterial supply to the renal remnant after double-layer suture of the renal defect.

For all three cases, the surgical strategy planning and intraoperative guidance based on 3DVMs are explained in the accompanying video.

2.4. Measurements

For each patient, demographic data including age, body mass index, comorbidities classified according to the Charlson-Deyo comorbidity index (CCI) and American Society of Anesthesiologists (ASA) score were collected [15,16]. Preoperative data included the tumor grade and reason for NSS indication, clinical size and stage, and tumor surgical complexity according to the PADUA score [17]. Intraoperative data considered the operative time, the duration of ischemia, the estimated blood loss, the conversion to radical nephrectomy and the intraoperative complications. Postoperative and pathological data included the length of hospital stay, 90-d postoperative complications classified according to the modified Clavien-Dindo system [18], pathological stage, histology, and grade. In addition, data on positive surgical margins were recorded. In terms of renal function, serum creatinine and eGFR were assessed preoperatively and 12 mo after surgery.

3. Results

Demographic data and perioperative characteristics are reported in Table 1. Two of the three patients harbored bilateral renal tumors. The third patient presented with a renal mass in the left kidney and contralateral renal hypoplasia (right SRF 25%). All the patients had similar anatomical and tumor features: the left kidney was affected by central highly complex tumor (PADUA 13), an accessory feeding artery and venous branch for the lower pole of the kidney, and a single long and narrow calyceal infundibulum draining the whole upper pole of the kidney, close to the renal mass. All three patients underwent 3DVM-assisted RAPN without intraoperative or postoperative complications. Final pathology revealed one chromophobe, one papillary, and one clear-cell renal cell carcinoma. No positive surgical margins were recorded. At 12 mo after surgery, the postoperative eGFR was 48, 33, and 55 ml/min for cases 1, 2, and 3, respectively. Except for case 2, who underwent postoperative dialysis for 6 mo, no further dialysis sessions were needed after surgery despite the heminephrectomy.

Table 1 – Descriptive characteristics of the three patients harboring complex left renal masses with an imperative indication for nephron-sparing surgery

Parameter	Case 1	Case 2	Case 3
Age at surgery (yr)	50	57	67
Body mass index (kg/m^2)	30	26	25
Charlson comorbidity index	2	2	3
American Society of Anesthesiologists score	2	2	3
Indication for nephron-sparing surgery	Imperative	Imperative	Imperative
Reason for imperative indication	Contralateral renal hypoplasia	Bilateral tumors	Bilateral tumors
Lesion size (mm)	80	70	55
Clinical stage	cT2a	cT1b	cT1b
PADUA nephrometry score	13	13	13
Ischemia time (min)	23.2	28.8	19
Estimated blood loss (cm^3)	550	350	375
Operative time (min)	117	148	120
Conversion to radical nephrectomy	No	No	No
Intraoperative complications	No	No	No
Postoperative Clavien grade >2 complications	No	No	No
Length of hospital stay (d)	6	12	5
Pathological stage	pT3a	pT3a	pT3a
RCC tumor histology	Chromophobe	Clear cell	Papillary type 1
ISUP grade group	NA	3	2
Surgical margins	Negative	Negative	Negative
Preoperative serum creatinine (mg/dl)	1.2	1.35	0.70
Preoperative eGFR (ml/min)	68	58	83
Postoperative serum creatinine at 12 mo (mg/dl)	1.63	2.20	0.99
Postoperative eGFR at 12 mo (ml/min)	48	33	55

eGFR = estimated glomerular filtration rate (Modification of Diet in Renal Disease formula); ISUP = International Society of Urological Pathology; RCC = renal cell carcinoma.

4. Discussion

Although most of the conservative surgeries now performed for organ-confined renal masses are elective, in some cases the indication for NSS is imperative [1–4].

In this context, it has been shown that both printed and virtual 3D models for preoperative planning and intraoperative navigation for NSS have a positive impact on postoperative outcomes [19–22]. Therefore, 3DVMs are increasingly being used for planning complex surgeries in routine practice [8,21] and pioneering studies have demonstrated the feasibility of 3D-AR guidance during RAPN to tailor tumor resection and renal reconstruction with the aim of achieving "precision RAPN" and maximizing postoperative functional recovery [10,12].

The accompanying video shows how 3DVM assistance can be used to modulate the type of NSS for high-complexity renal masses with an imperative indication for NSS.

In the first case demonstrated, the surgeon performs an enucleoresection, although, as observed for the other two cases, a heminephrectomy would have been the optimal choice.

The reasoning for this surgical strategy came from careful evaluation of 3DVMs, which were essential for identification of a specific "anatomical cluster": for all three patients, virtual images demonstrated a left kidney affected by a central highly complex tumor, with an accessory feeding artery and venous branch for the lower pole of the kidney and a single long and narrow calyceal infundibulum draining the whole upper pole of the kidney, in intimate contact with the renal mass.

The surgical strategy suggested by 3DVM evaluation was therefore sacrifice of the parenchyma of the upper calyx in a heminephrectomy procedure. The rationale was that this choice might have lower perioperative risks (arterial-venous fistulas/pseudoaneurysms, urine leakage, hydrocalyx formation) balanced against a high probability of functional benefits versus a surgical strategy in which the risk of complications is potentially higher and the functional advantages are doubtful for anatomical reasons. In fact, the risk of upper calyceal infundibulum violation or injury during surgical resection of a tumor adhering to the tubular structure is not negligible, exposing the patient to the risk of postoperative urine leakage and, at the same time, excluding a significant proportion of functionally active parenchyma from the collecting system and leading to death of the excluded renal units.

This reasoning based on an anatomic-functional perspective was confirmed by postoperative evidence. In case 1, we observed full functional loss of the upper portion of the kidney, in which the spared parenchyma was lost due to hydrocalyx-derived compression. Conversely, the renal remnant in cases 2 and 3 was vascularized and functioning well, as demonstrated by intraoperative ultrasound and ICG injection. For the latter two cases, preservation of an independent vascular and collecting unit allowed return of urine production and output and good functional recovery.

The role of 3DVMs in planning NSS surgical strategies in the case of particular anatomical clusters has been investigated in other studies. Campi et al [23] presented a case report on a 74-yr-old Caucasian male with incidental detection of two complex renal masses in the left portion of a horseshoe kidney. They concluded that 3DVM assistance allows optimization of postoperative outcomes by ensuring that proper surgical experience and careful preoperative planning are in place, and tailoring surgical strategies and techniques according to the individual patient's anatomy.

As suggested by their work and confirmed by our study, a great advantage of 3DVM assistance during preoperative planning for complex RAPNs, especially in challenging scenarios such as imperative indications for NSS, is the ability to conduct a "virtual" surgery before performing the procedure in the operating room.

Although this novel technology seems promising for defining specific anatomical clusters and planning the surgical strategy, the current study is not devoid of limitations. First, the case series is limited in sample size. Second, 3D model segmentation of the kidney and tumors was performed manually; an experienced urologist and an experienced radiologist were needed to complete the segmentation process. Third, intraoperative overlapping was performed by an assistant using a 3D mouse to set the proper orientation of the virtual model over the real anatomy. Future evolution of this technology, already tested in some preliminary experiences, will be the development of software that can automatically anchor the virtual model to the intraoperative images regardless of surgeon or camera movements [24]. Fourth, to assess the real benefits of 3D-AR technology for complex renal masses with an imperative indication for NSS, a prospective randomized study and larger sample sizes are required.

Despite these limitations, our study is the first to show the real impact of 3DVMs in defining a specific functional anatomical cluster and planning the optimal surgical strategy that is well balanced between perioperative risks and effective functional benefits.

5. Conclusions

For complex renal masses with an imperative indication for NSS, 3DVMs facilitate planning of the surgical strategy considering the specific anatomy of the kidney. 3DVMs increase the surgeon's ability to identify specific anatomical clusters and therefore to focus attention on the effective functional gain of the intervention, and even to consider sacrificing portions of the organ that can technically be preserved but are functionally not useful.

Author contributions: Francesco Porpiglia had full access to all the data in the study and takes responsibility for the integrity of the data and the accuracy of the data analysis.

Study concept and design: Amparore, Piramide, Pecoraro, Checcucci, Porpiglia.
Acquisition of data: Verri, De Cillis, Piana, Busacca.
Analysis and interpretation of data: Amparore, Piramide, Pecoraro, Verri, Porpiglia.
Drafting of the manuscript: Amparore, Piramide, Pecoraro, Verri.
Critical revision of the manuscript for important intellectual content: Amparore, Piramide, Pecoraro, Manfredi, Fiori, Porpiglia.
Statistical analysis: Pecoraro.
Obtaining funding: None.
Administrative, technical, or material support: Fiori.
Supervision: Porpiglia.
Other: None.

Financial disclosures: Francesco Porpiglia certifies that all conflicts of interest, including specific financial interests and relationships and affiliations relevant to the subject matter or materials discussed in the manuscript (eg, employment/affiliation, grants or funding, consultancies, honoraria, stock ownership or options, expert testimony, royalties, or patents filed, received, or pending), are the following: None.

Funding/Support and role of the sponsor: None.

Appendix A. Supplementary data

Supplementary data to this article can be found online at https://doi.org/10.1016/j.euros.2022.02.006.

References

[1] Leslie S, Goh AC, Gill IS. Partial nephrectomy—contemporary indications, techniques and outcomes. Nat Rev Urol 2013;10:275–83.
[2] Brassetti A, Anceschi U, Bertolo R, et al. Comprehensive long-term assessment of outcomes following robot-assisted partial nephrectomy for renal cell carcinoma: the ROMe's achievement and its predicting nomogram. Minerva Urol Nefrol 2020;72:482–9.
[3] Long JA, Bernhard JC, Bigot P, Lanchon C, et al. Partial nephrectomy versus ablative therapy for the treatment of renal tumors in an imperative setting. World J Urol 2017;35:649–56.
[4] Tan JS, Sathianathen N, Cumberbatch M, Dasgupta P, et al. Outcomes in robot-assisted partial nephrectomy for imperative vs elective indications. BJU Int 2021;128(Suppl 3):30–5.
[5] Amparore D, Pecoraro A, Piramide F, et al. Comparison between minimally-invasive partial and radical nephrectomy for the treatment of clinical T2 renal masses: results of a 10-year study in a tertiary care center. Minerva Urol Nephrol 2021;73:509–17.
[6] Buffi NM, Saita A, Lughezzani G, et al. Robot-assisted partial nephrectomy for complex (PADUA score ≥10) tumors: techniques and results from a multicenter experience at four high-volume centers. Eur Urol 2020;77:95–100.
[7] Veccia A, Dell'Oglio P, Antonelli A, et al. Robotic partial nephrectomy versus radical nephrectomy in elderly patients with large renal masses. Minerva Urol Nefrol 2020;72:99–108.
[8] Bertolo R, Autorino R, Fiori C, et al. Expanding the indications of robotic partial nephrectomy for highly complex renal tumors: urologists' perception of the impact of hyperaccuracy three-dimensional reconstruction. J Laparoendosc Adv Surg Tech A 2019;29:233–9.
[9] Checcucci E, Amparore D, Pecoraro A, et al. 3D mixed reality holograms for preoperative surgical planning of nephron-sparing surgery: evaluation of surgeons' perception. Minerva Urol Nephrol 2021;73:367–75.
[10] Porpiglia F, Checcucci E, Amparore D, et al. Three-dimensional augmented reality robot-assisted partial nephrectomy in case of complex tumours (PADUA ≥10): a new intraoperative tool overcoming the ultrasound guidance. Eur Urol 2020;78:229–38.
[11] Porpiglia F, Amparore D, Checcucci E, et al. Three-dimensional virtual imaging of renal tumours: a new tool to improve the accuracy of nephrometry scores. BJU Int 2019;124:945–54.
[12] Amparore D, Pecoraro A, Checcucci E, et al. Three-dimensional virtual models' assistance during minimally invasive partial nephrectomy minimizes the impairment of kidney function. Eur Urol Oncol 2021. https://doi.org/10.1016/j.euo.2021.04.001, In press.
[13] Rossanese M, Crestani A, Giannarini G, et al. Absolok® versus Hem-o-Lok® clips for renorrhaphy during partial nephrectomy for parenchymal renal tumors. Minerva Urol Nefrol 2020;72:91–8.
[14] Diana P, Buffi NM, Lughezzani G, et al. The role of intraoperative indocyanine green in robot-assisted partial nephrectomy: results from a large, multi-institutional series. Eur Urol 2020;78:743–9.
[15] Charlson ME, Pompei P, Ales KL, MacKenzie CR. A new method of classifying prognostic comorbidity in longitudinal studies: development and validation. J Chronic Dis 1987;40:373–83.
[16] Ament R. Origin of the ASA classification. Anesthesiology 1979;51:179.
[17] Ficarra V, Novara G, Secco S, et al. Preoperative aspects and dimensions used for an anatomical (PADUA) classification of renal tumours in patients who are candidates for nephron-sparing surgery. Eur Urol 2009;56:786–93.
[18] Dindo D, Demartines N, Clavien PA. Classification of surgical complications: a new proposal with evaluation in a cohort of 6336 patients and results of a survey. Ann Surg 2004;240:205–10.
[19] Porpiglia F, Bertolo R, Checcucci E, et al. Development and validation of 3D printed virtual models for robot-assisted radical prostatectomy and partial nephrectomy: urologists' and patients' perception. World J Urol 2018;36:201–7.
[20] Shirk JD, Thiel DD, Wallen EM, et al. Effect of 3-dimensional virtual reality models for surgical planning of robotic-assisted partial nephrectomy on surgical outcomes: a randomized clinical trial. JAMA Netw Open 2019;2:e1911598.
[21] Porpiglia F, Fiori C, Checcucci E, Amparore D, Bertolo R. Hyperaccuracy three-dimensional reconstruction is able to maximize the efficacy of selective clamping during robot-assisted partial nephrectomy for complex renal masses. Eur Urol 2018;74:651–60.
[22] Cacciamani GE, Okhunov Z, Meneses AD, et al. Impact of three-dimensional printing in urology: state of the art and future perspectives. A systematic review by ESUT-YAUWP group. Eur Urol 2019;76:209–21.
[23] Campi R, Sessa F, Rivetti A, et al. Case report: optimizing pre- and intraoperative planning with hyperaccuracy three-dimensional virtual models for a challenging case of robotic partial nephrectomy for two complex renal masses in a horseshoe kidney. Front Surg 2021;8:665328.
[24] Amparore D, Checcucci E, Piazzolla P, et al. Indocyanine green drives computer vision based 3D augmented reality robot assisted partial nephrectomy: the beginning of "automatic" overlapping era. Urology 2021. https://doi.org/10.1016/j.urology.2021.10.053, In press.